On-demand Delivery of Single DNA Molecules Using Nanopipettes

Aleksandar P. Ivanov[1,*] Paolo Actis[2,*], Peter Jönsson[3,4,*], David Klenerman[4], Yuri Korchev[2], Joshua B. Edel[1,#]

1 Department of Chemistry, Imperial College London, SW7 2AZ, United Kingdom

2 Department of Medicine, Imperial College London, W12 0NN, United Kingdom

3 Department of Chemistry, Lund University, SE-221 00, Sweden

4 Department of Chemistry, University of Cambridge, CB2 1EW, United Kingdom

[*] These authors contributed equally to this work

[#] corresponding author: joshua.edel@imperial.ac.uk

Keywords

Single-molecule delivery, label-free detection, nanopore, nanopipette, DNA

Abstract

Understanding the behavioral properties of single molecules or larger scale populations interacting with single molecules is currently a hotly pursued topic in nanotechnology. This arises from the potential such techniques have in relation to applications such as targeted drug delivery, early stage detection of disease, and drug screening. Although label and label-free single molecule detection strategies have existed for a number of years, currently lacking are efficient methods for the controllable delivery of single molecules in aqueous environments. In this article we show both experimentally and from simulations that nanopipettes in conjunction with asymmetric voltage pulses can be used for label-free detection and delivery of single molecules through the tip of a nanopipette with "on-demand" timing resolution. This was demonstrated by controllable delivery of 5 kbp and 10 kbp DNA molecules from solutions with concentrations as low as 3 pM.

Rapid single-molecule detection and controllable single-molecule delivery are two of the central themes of modern nanotechnology. Unfortunately these themes are often disconnected, particularly in environments which require physiological and label-free conditions. A class of versatile single-molecules detectors – nanopores or nanopipettes, has shown exceptional promise for label-free analysis of key life components such as DNA, RNA, and proteins,[1-10] but has not been used for controllable delivery of biomolecular species. The ability to simultaneously deliver and analyze individual molecules in label-free conditions, is one of the ultimate goals in nanotechnology and can open up avenues for the quantitative analysis of biological, chemical and physical phenomena on an individual non-statistical basis. However, at the single molecule level, the analyte transport (and detection) across the nanopore is typically a random process, resulting in limited control on the transport of individual molecules.

In a typical nanopore sensing platform, two reservoirs containing electrolyte are connected *via* a nanoscale pore. Voltage is applied across the nanopore to generate a steady-state ionic current that depends on the pore dimensions, charge, and the ionic strength of the solution.[1, 3] Analytes are electrokinetically translocated through the nanopore and are detected by transient variations in the ionic current. A sub-class of nanopores, used in this work, is nanopipettes. Importantly, they can be rapidly and inexpensively laser pulled from glass capillaries, resulting in a sharp tip constituting a single nanopore, which can be used as single-molecule label-free sensors,[10-14] in the same way as conventional solid-state nanopores. Due to their high-aspect ratio geometry and exceptionally sharp tips, nanopipettes offer an important advantage over conventional nanopores as they can be easily adapted for use in single cell interrogation[15, 16] and as a macroscopic delivery vehicle for intracellular injection.[17-22]. To date, delivery of molecules has so far only been quantified in close proximity to the tip by using fluorescence

spectroscopy.[18, 21, 23] Real-time quantitative delivery of *individual molecules* combined with label-free nanopore detection has yet to be achieved. In fact nanopipettes are predominantly used as an analytical platform for the detection of single molecules by transporting molecules from the outside reservoir to the inside of the nanopipette.[10, 12, 13, 24-27]. However, this does not take advantage of utilizing the nanopipette as a label-free single-molecule delivery vehicle.

Here, we address this fundamental gap and report on simultaneous label-free detection and on-demand delivery of single DNA molecules with nanopipettes, with precise control of the time of delivery and the number of delivered molecules. Molecular delivery is demonstrated down to picomolar concentrations ($<10^6$ DNA molecules in sub-microliter volumes), advancing high-sensitivity detection and delivery of unamplified samples using nanopipettes. Additionally, molecules can be controllably transported back and forth prior to reaching the tip of the nanopipette by using asymmetric voltage pulses, acting as an "on-off switch" for on-demand molecular delivery. Ultimately, we envision applications in controllable delivery of individual oligonucleotides (inside living cells), providing new insights in processes such as gene regulation and infection, and single-molecule PCR, to mention a few examples.

Results and Discussion

A schematic of the principle behind the experiment is shown in Figure 1a. Quartz nanopipettes were fabricated by laser-assisted pulling as described in the Methods section. The nanopipettes used in this study had a resistance of 250±35 MΩ (as measured in a low bias (−0.1 V; 0.1 V) regime in 0.1 M KCl, 10 mM Tris/EDTA, pH 8) and a nanopore diameter of 25±4 nm, as determined by SEM (Fig. 1cb). All nanopipettes exhibited $I_{-500\ mV}/I_{500\ mV}$ = 1.6±0.4 (Fig. 1c), consistent with the rectification behavior observed in negatively charged conical geometries.[28-31]

The nanopipettes were filled with (5 kbp or 10 kbp) double-stranded DNA solution and Ag/AgCl electrodes were fitted both in the nanopipette (patch electrode) and in the external reservoir containing only buffer (bath/ground electrode). Under these conditions, the negatively charged DNA molecules inside the nanopipette migrate toward the inner electrode under positive applied potentials and toward the tip of the nanopipette under negative potentials. In contrast to traditional nanopore experiments where a constant DC voltage is applied, we used periodic pulses of positive (V^+) and negative (V^-) potentials with durations t^+ and t^-, respectively. This allowed us to minimize clogging of the nanopipette,[32] and importantly, to deliver individual DNA molecules through the tip of the nanopipette in a controllable manner (schematic Fig. 1a). We observed that in each pulse, the time between the application of V^- and the detection of the first translocation event (dT) was remarkably regular and could be controlled by varying the magnitude of V^-, V^+ and t^+. Figure 2a shows representative time traces for voltage (V-t) and current (I-t) during 500 seconds (24 consecutive delivery pulses) for delivery from one of the DNA solution used (150 pM, 10 kbp DNA). During a V^- pulse individual DNA molecules are delivered and detected as transient changes of the ionic current as shown in Fig. 2b (zoomed in views of several representative delivery events for 10 kbp and 5kbp DNA are available in Supporting Fig. 1). At 0.1 M KCl, the translocation of DNA through the tip of the nanopipette elicits a temporary increase in the conductance rather than a decrease. This effect is due to conducting counter ions that shield the negatively charged phosphate backbone of the translocated DNA molecule, which has been observed before in similar ionic strength conditions.[24, 33] The high reproducibility in the measured current between each delivery pulse can be used to combine single-molecule detection statistics from each pulse in all event histograms. Histograms and event scatter plots of peak current caused by translocations, ΔI vs dwell time and

equivalent charge (integrated current area per translocation) vs dwell time are shown in Fig. 2c, indicating that the most of the DNA molecules are in an unfolded state when being translocated through the tip of the nanopipette.[12] This is also in agreement with the observation of translocation events as single steps in the ioninc current as shown in Supporting Fig. 1. Based on calculations from the histogram fits, at V^- = -300 mV the most probable dwell time was 0.6±0.2 ms with a mean equivalent charge of 18.0±4.1 fAs. Both values are in good agreement with previously reported data for 10 kbp DNA molecules, albeit in those experiments DNA molecules were translocated from the external reservoir to the inside of the nanopipette.[26, 27]

The reproducibility of the molecular delivery between individual pulses is illustrated in Fig. 2d, 2e, and 2f for V^- = -200 mV, -300 mV and -400 mV, respectively. *I-t* traces of 15 representative V^- pulses (5 for each potential) are shown in panels (i) in Fig. 2d, 2e, and 2f, demonstrating a well-defined 'time of arrival' dT, for the delivery of the first molecule in each V^- pulse, with a small spread in the delivery time of approximately the same magnitude as the average time between successive delivery events δt. Panels (ii) in Fig. 2d, 2e, and 2f shows the number of molecules delivered per pulse for 24 consecutive pulses (total duration of 500 s). The average number of molecules delivered per pulse was 17.7 ± 4.5 at V^- = -400 mV, 13.1 ± 3.3 molecules at V^- = -300 mV and 8.0 ± 3.0 molecules at V^- = -200 mV. Panels (iii) illustrate the controllable delivery of the first molecule with a histogram of dT showing the distribution of the time of the first event. The first molecule is delivered faster for higher V; for 10 kbp DNA molecules with t^+ = 6.4 s and V^+ = 500 mV, the time of the first event dT was 2.9 ±0 .6 s, 3.8 ± 1.1 s and 6.2 ±0 .9 s for V^- = -400 mV, -300 mV and -200 mV, respectively. All error estimates are standard deviations. These results are not device-dependent in the sense that they have been reproduced with over 30 nanopipettes fabricated with the same laser puller settings.

Experiments analogue to the ones shown in Fig. 2 have been performed for 5 and 10 kbp DNA for a range of concentrations (3 pM to 1500 pM) and negative potentials V^- (-200 mV to -500 mV). Scatter plots and histograms showing delivery and detection of 5 kbp DNA molecules are available in Supporting Fig. 2. It was possible to reliably deliver and detect both 5 and 10 kbp DNA molecules from concentrations as low as 3 pM (equal to 3 attomol of DNA sample in the nanopipette volume of ~1 μl), demonstrating the suitability of the method for the delivery and detection from ultra-small sample volumes, without the need of amplification. These results indicate detection sensitivity that is directly comparable to ultra-low concentration detection (3.8 pM DNA) only accomplished with high salt gradients across the nanopore.[4] Multiple single-molecule delivery data has been summarized in Supporting Fig. 3 as measurements of 5 and 10 kbp DNA capture rates as a function of V^- at concentrations varying from 3 pM to 1500 pM. To avoid potential recapture of the already translocated DNA molecules,[34, 35] a delay step of 0.6 s at 0 V was introduced between each delivery pulse (0.3 s before a V^+ pulse and after the V^- pulse). Gershow and Golovchenko, have shown that the probability of recapture decreases dramatically with the time elapsed before the application of a reverse potential (V^+ here).[34] Indeed, recaptured DNA molecules were not observed in the V^+ current time traces as show in Supporting Fig. 4.

The transport of DNA through the nanopipette under pulsed potentials can in the first instance be described as the interplay of electrophoretic (EP) and electroosmotic (EO) forces, where DNA molecules are pulled back and forth along the nanopipette. For the current conditions the dominating force will be due to EP. In a V^+ pulse, the electroosmotic flow is directed from the inside to the outside of the nanopipette, while EP pulls DNA molecules that are already close to the tip towards the nanopipette interior. The DNA molecules, which are initially randomly distributed inside the nanopipette, (except very close to the tip (~2 μm), where they are

excluded, due to sterical restraints), get pulled along the nanopipette axis to a distance z from the tip, depending on the duration of positive pulse (t^+). When a negative pulse V^- is applied (at the time $t=t^+$) the electroosmotic flow is directed into the nanopipette, while EP moves the DNA molecules towards the nanopore. For negative pulses with sufficiently long duration ($t^->dT$), the DNA molecules have enough time to travel the distance z to the nanopore followed by delivery. This mechanism is the basis of the controllable delivery and was confirmed by fluorescence imaging of labelled DNA at the nanopipette tip (Fig. 3, Supporting Fig. 5 and movie DNATrans.avi in Supporting Information) and finite element simulations (Supporting Fig. 6), in addition to the presented ionic current data.

To estimate the rate of transport of DNA in the nanopipette, the following approximate expression is used:

$$C_{\mathrm{R}} = \frac{\mu_{\mathrm{ep}} I}{K} C + Q_{\mathrm{eo}} C \qquad (1)$$

where C_{R} is the average number of DNA molecules passing a cross-section of the nanopipette per second (equal to the average capture rate at the nanopore), C is the concentration of DNA in the nanopipette, μ_{ep} is the electrophoretic mobility of the DNA, I is the ion current, K the (bulk) ion conductivity and Q_{eo} the electroosmotic flow. This expression is based on the assumption of having, on average, the same amount of DNA molecules passing each cross section of the nanopipette. This is equivalent of having no local accumulation or depletion of DNA molecules in the nanopipette, an assumption that is supported by fluorescence imaging of DNA in the nanopipette (Fig. 3). Even if the concentration of ions close to the tip of the nanopipette is changing under conditions of ion rectification, the concentration far from the tip should be independent of the sign of the applied voltage[36, 37] and the electric field in that region can be estimated by $I/(A\times K)$, where A is the cross-sectional area of the nanopipette in the studied region.

The exact values of the terms in eq (1) close to the tip might be different, and other forces such as dielectrophoresis might also act on the DNA molecules in this region,[38] but since the transport of the DNA molecules is mainly taking place in the region far from the tip (see Supporting Fig. 8 and movie DNATrans.avi) this effect can mainly be neglected for the current experiments.

Finite element simulations were performed in COMSOL Multiphysics 4.3b to estimate I and Q_{eo} under different applied voltages (c.f. the Methods section and the Supporting Fig. 6 and 7) for the same nanopipette geometry as measured optically and by SEM. The time to the first event, dT, can, as a first approximation, be estimated by the following expression (see Supporting Information for details):

$$dT = -\frac{\left(\mu_{ep} I_{+} + KQ_{eo,+}\right)}{\left(\mu_{ep} I_{-} + KQ_{eo,-}\right)} t_{+} \qquad (2)$$

where the +/- signs indicate the ion current and the electroosmotic flow rate for the positive/negative pulses. Inserting the simulated values for the ion current and the electroosmotic flow (Supporting Fig. 6b,c) gives dT as a function of V^-, V^+ and t^+ only. Figure 4a shows experimentally measured dT for different V^- (for V^+ = 500 mV and t^+ = 6.4 s) based on 643 delivery cycles for 5 kbp and 10 kbp DNA molecules with a concentration of 30 pM and 150 pM. The experimentally measured dT values were found to be in relatively good agreement with the estimated values from eq (2) (dashed lines in Fig. 4a), showing an increase in the delivery time with lower voltages V^- due to a lower flux of DNA in the nanopipette. However, eq (2) does not describe the dependency of dT with the concentration of DNA in the nanopipette and the length of the DNA molecules, which from Fig. 4a is seen to have an effect on the delivery time. To investigate this and to estimate the spread in the delivery times, we performed time-dependent finite elements simulations of the delivery during a voltage cycle (for details see

Methods section and Supporting Fig. 8). The results of these simulations are shown as solid lines in Fig. 4a (and Fig. 4c) and are in good agreement with the experimental values. The average delivery time decreases when the concentration of DNA molecules increases (Fig. 4a). An explanation to this behavior is that, due to the random distribution of DNA molecules in the nanopipette at $t = 0$, the DNA molecule closest to the tip of the nanopipette is on average further away from the tip at $t = 0$ for lower concentrations compared to higher concentrations. These DNA molecules will therefore travel further into the nanopipette during the positive voltage pulse, and will exit the nanopipette at a later time dT (see also Supporting Fig. S9). There will also be a higher likelihood of a DNA molecule having diffused (a longer distance) towards the tip of the nanopipette when the concentration is increased, thus resulting in a lower dT. This will also be affected by the diffusivity of the molecule, which is why shorter (5Kb) DNA molecules have slightly lower dT than the longer (10Kb) DNA molecules (see Fig. 4a).

The time of delivery can also be adjusted by varying the positive pulse duration t^+. Figure 4b provides a plot of dT values measured in 340 delivery cycles with $V^+ = 500$ mV, $V^- = -300$ mV and $t^- = 21$ s as a function of t^+ together with data from the time-dependent simulations, showing an excellent agreement between experimental and simulated data. The value for dT is initially increasing linearly with t^+ as predicted from eq (2), in agreement between the measured slope ($dT/t^+ = 0.69 \pm 0.03$) and the one calculated from eq (2) ($dT/t^+ = 0.71$). The delivery time is decreasing at higher t^+ due to increased diffusion when the DNA is transported further into the nanopipette. In summary, both the theoretical and experimental results demonstrate that, for a constant value of V^-, the precise time of the delivery of the first molecule can be controlled by the duration of the positive potential t^+. While molecular delivery occurs when negative pulses

are applied, decreasing the duration of the positive pulse t^+ results in quicker delivery of the first molecule.

The number of DNA molecules delivered per pulse, N, is given by:

$$N = C_R\left(t^- - dT\right) \tag{3}$$

Together with eqs (1) and (2), the number of molecules delivered in a negative pulse with a set duration t^- is proportional to the analyte concentration C. The number of delivered molecules can be controlled by varying dT , V^- (see Fig. 4c), V^+ or t^+ (see Fig. 4d). Fig. 4c shows that varying V^- has two effects: (i) an increase of V^- results in a higher capture rate C_R (see eq (1)) thus increasing the number of DNA molecules delivered and (ii) an increase in V^- reduces the time dT thus leading to a larger time (t^- - dT) for delivery and more DNA molecules being delivered. Figure 4d shows the variation of the number of delivered DNA molecules with different values of t^+. Since C_R is independent of t^+ (and t^-), as measured experimentally and shown in the inset in Fig. 4d, the only time dependence in N is in the term (t^- - dT) (see eq (3)). Since dT is proportional to t^+ (as indicated by eq (2) and experimentally shown in Fig. 4b), the total number of delivered molecules will also decrease linearly with t^+ as shown in the experimental and the theoretical data in Fig. 4d.

These findings further confirm that during alternating pulses DNA molecules are transported back and forth close to the nanopipette tip and demonstrate that the potentials V^+ and V^-, as well as the pulse duration t^+, can be used to actively control the delivery of a defined number of DNA molecules. The control over dT can further be used for the precise delivery of individual molecules in a single pulse. The negative pulse duration t^- can be set such that on average only one molecule is delivered in a pulse (as shown in several consecutive pulses in Fig.

5a). The latter is also demonstrated in Fig. 5b$_i$ to b$_{iii}$ for three different combinations of t^+ and t^- (with up to 75 delivery pulses each), chosen for values of dT such that $N = 1$ as predicted from the time-dependent simulations and from eqs (2) and (3). It should be noted, that prior to applying voltage pulses the DNA molecules are randomly distributed in the nanopipette and the probability density function of finding a DNA molecule is assumed to be the same at all position in the nanopipette. This will not be true close to the tip of the nanopipette (within ~2 μm from the tip), where in the absence of voltage pulses, the DNA molecules will be excluded due to sterical constraints. Since the DNA molecules for the majority of the delivery cycle are further away than this distance, this can be used as a first approximation. From the random distribution of DNA in the nanopipette at $t = 0$ it is thus expected that the delivery should also contain a spread in dT, and that the number of molecules being delivered after a time t^- to follow a Poisson distribution. Comparing experimental results versus simulated predictions based on Poisson statistics for the number of molecules delivered per cycle for different combinations of t^+ and t^-, generally shows good agreement, which states a maximum likelihood of one DNA molecule being delivered of $1/e \approx 0.37$. However, it should be mentioned that delivery situations also occur, which are very unlikely based on Poisson statics. An example of this deviation is shown in Fig. 5a where 13 single molecule delivery events out of 16 consecutive pulses are observed. The likelihood of this occurring is less than 1 in 5000. It is thus possible that other effects, such as confinement or steric exclusion at and near the tip of the nanopipette, can affect the delivery, resulting in a higher likelihood of getting single delivery event than expected from Poisson statistics.

Since dT is proportional to t^+, it is possible to deliver single molecules in a short pulse with a low dT, just by varying t^+ (as can be seen from the pulse durations in Fig. 5b). Additional

experimental data (plots of dT distribution and the number of molecules delivered per cycle) for a constant t^+ (hence a constant dT), showing, as predicted, an increase of the number of molecules delivered per cycle with increasing t^-, are available in Supporting Fig. 10.

The control over dT can further be used in the regime $t^- < dT$, to repeatedly pulse molecules in the nanopipette, back and forth close to the nanopore, without delivering the molecule. Molecular delivery can thus be switched on-demand for $t^- > dT$, to deliver a specific number of molecules (Fig. 5c_i) or a single molecule by controlling dT (Fig. 5c_{ii}). In principle, the experimental regimes presented in Fig. 5a,c_{ii} can be combined to alternate between pulsing a molecule close to the tip and on-demand delivery of a single molecule. This unique capabilities of on-demand, switchable molecular delivery and simultaneous label-free detection can serve as a particularly powerful tool in studies with living cells. The nanopipettes used in this work can be integrated with ion conductance microscopy to scan ($t^- < dT$) the surface of living cells and perform targeted delivery on demand ($t^- > dT$) in a cell area of choice. Another exciting application is possibility of using the region inside the nanopipette, near the tip as an ultra-small reaction volume,[39] where small molecular populations are pulsed back and forth and interact with each other, with the reaction products simultaneously delivered and detected by the nanopore.

Conclusions

In this article we showed controllable delivery of single DNA molecules with simultaneous label-free detection. We demonstrated that even highly diluted unamplified molecular populations can be efficiently delivered with control of the time of delivery of the first molecule and the number of molecules delivered. We believe that these findings can open the door to using nanopipettes as a single molecule delivery tool, which is expected to have a broad

range of applications, including targeted delivery of nucleic acids, gene regulation, infection, and single molecule PCR.

Methods

Nanopipette fabrication

Nanopipettes were fabricated using a P-2000 laser puller (Sutter Instrument Co) from quartz capillaries with an outer diameter of 1.0 mm and an inner diameter of 0.5 mm (QF100-50-7.5; Sutter Instrument Co).

Nanopipettes were fabricated using a two-line protocol: 1) HEAT: 575; FIL: 3; VEL: 35; DEL: 145; PUL: 75, followed by 2) HEAT: 900; FIL: 2; VEL: 15; DEL: 128; PUL: 200. It should be noted that the pulling protocol is instrument specific and there is variation between P-2000 pullers.

DNA solutions

Double stranded DNA with lengths 5 kbp and 10 kbp and with a stock concentration of 500 μg/ml were obtained from New England Biolabs. DNA filling solutions (3 pM, 30 pM, 150 pM and 1500 pM) were prepared by serial dilution. The filling concentrations were cross-checked with a NanoDrop 2000c UV-Vis spectrophotometer (Thermo Fisher Scientific Inc.). Each nanopipette was filled once and used with only one solution. Nanopipettes once used in an experiment were not reused.

Finite element simulations

Finite element simulations were performed in COMSOL Multiphysics 4.3b to model the electric field, the ion current and the electroosmotic flow in a nanopipette with R_0 = 12 nm, θ = 3.5° and $R_1 = 2R_0$. Similar simulations have previously been done for nanopores[36,37] and for nanopipettes.[31] The geometry used for the simulations is shown in Supporting Fig. 6. The surface charge of the nanopipette walls, σ, was estimated for 0.1 M KCl (conductivity of $K \approx 1.5$ S/m) as:

$$\sigma = \kappa \varepsilon_r \varepsilon_0 \zeta \tag{4}$$

where κ is the inverse Debye length, ε_r the relative permittivity of the solution, ε_0 the permittivity of vacuum and ζ the zeta potential of the nanopipette walls. The zeta potential for glass in a 0.1 M K^+ solution is approximately -30 mV (see ref.[40]) resulting in a surface charge of -22 mC/m^2. COMSOL Multiphysics was also used to solve the time-dependent diffusion/transport equation to in detail model the transport of DNA back and forth in the nanopipette during a voltage cycle (see Supporting Fig. 6 and Fig 7 for the simulation geometry). The nanopipette was assumed to be homogenously filled with DNA molecules at t = 0 and thus that the probability density function, c, of finding the DNA was the same at any position in the nanopipette. The distribution of c was then determined at subsequent times and the molecular/probability flux of DNA out of the nanopipette was calculated and used to determine the time of delivery of a single DNA molecule, and the delivery probability. Further details on the simulations are given in the Supporting Information together with theoretical formulas of how the simulated data was converted into values of dT and delivery probabilities.

Ionic current detection

The ion current was measured using a MultiClamp 700B or AxoPatch 200B patch-clamp amplifier (Molecular Devices, USA) in "voltage clamp" mode. The signal was filtered using a low-pass filter at 10 kHz and digitized with an Axon Digidata 1322A or Digidata 1440 at 50 kHz rate and recorded using the software pClamp 8/10 (Molecular Devices). Data analysis was carried out using a custom-written MATLAB analysis routine. The baseline current was calculated via moving window for every 5 data points. Peak current was calculated as current peak maximum after subtraction of the baseline current.

Fluorescence detection

The DNA stock solutions were labeled with YOYO-1 (Molecular Probes) at a ratio of 7.5 base pairs per dye molecule. Detection of DNA was achieved using a custom-built confocal microscope with imaging capabilities.[41, 42] Briefly, the excitation light from a 488 nm continuous wave laser was expanded on the nanopipette tip using a 60× objective). Fluorescence originating from DNA molecules transported along the tip and translocating through the nanopore was collected by the same objective and directed to an electron multiplying CCD (emCCD) camera (Cascade II, Photometrics). The camera has a pixel size of 16 μm, however, when used in conjunction with the 60× objective, generates an effective pixel size of 266 nm.

Figures

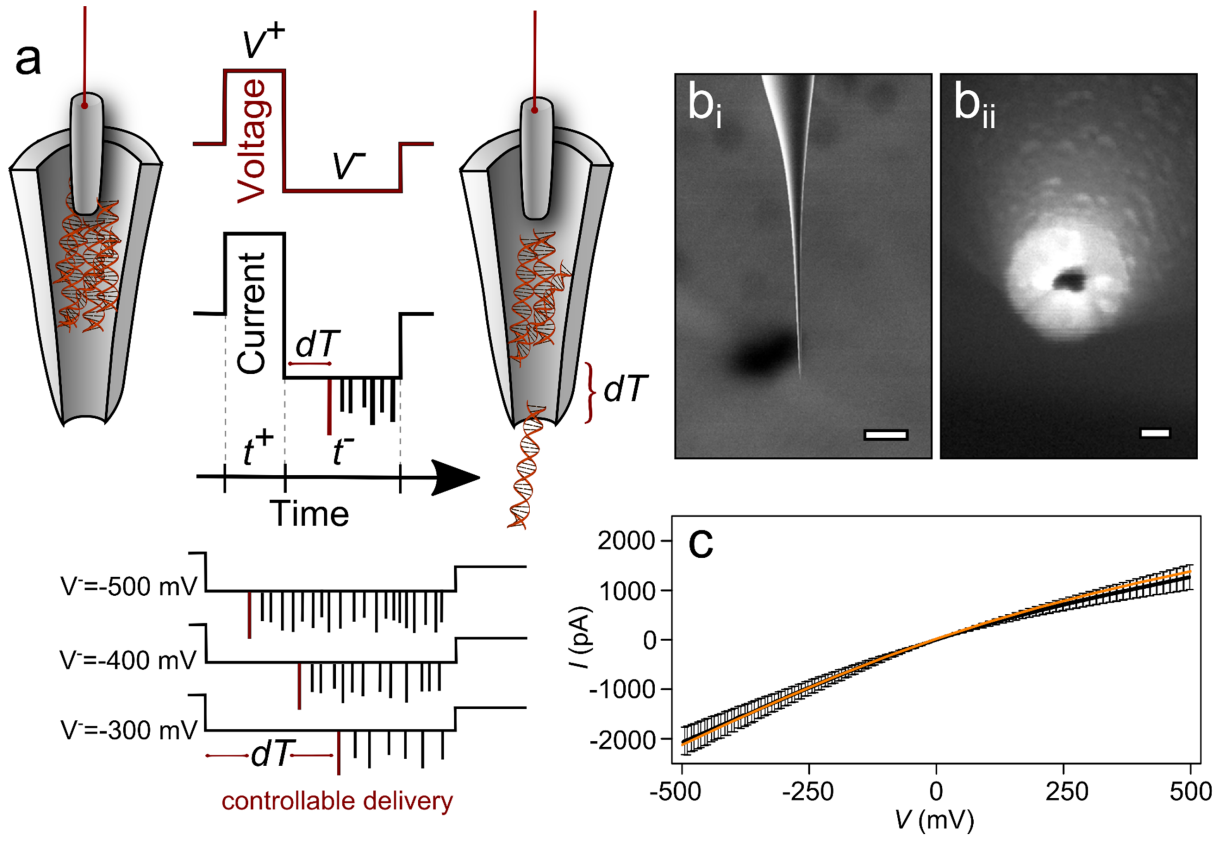

Figure 1 | Controlled delivery with a nanopipette delivery system. a, Schematic illustration showing the nanopipette delivery system. Positive (V^+) and negative (V^-) voltage pulses are applied for t^+ and t^-, respectively. Single DNA molecules are delivered during a (V^-) pulse and are detected as transient changes in the ion current. **b**, SEM images of the nanopipette tip (**b$_i$**) and the nanopore at the tip (**b$_{ii}$**). The scale bars are 250 µm and 25 nm, respectively. The nanopipettes had an inner half-cone angle of θ =3.5° resulting in a high length to width ratio of the nanopipette tip. **c,** Average *I-V* curves of 10 nanopipettes measured in 0.1 M KCl (black). The average ionic resistance was R = 250±35 MΩ. All nanopipettes exhibited ion current rectification with a ratio $I_{-500\ mV}/I_{500\ mV}$ = 1.6±0.4. The orange line is an *I-V* curve calculated by finite element

simulations in COMSOL Multiphysics by modeling the electric field, ion current and electroosmotic flow in the nanopipette as described in the Methods section. The simulated rectification ratio is $I_{-500\ mV}/ I_{500\ mV} = 1.5$.

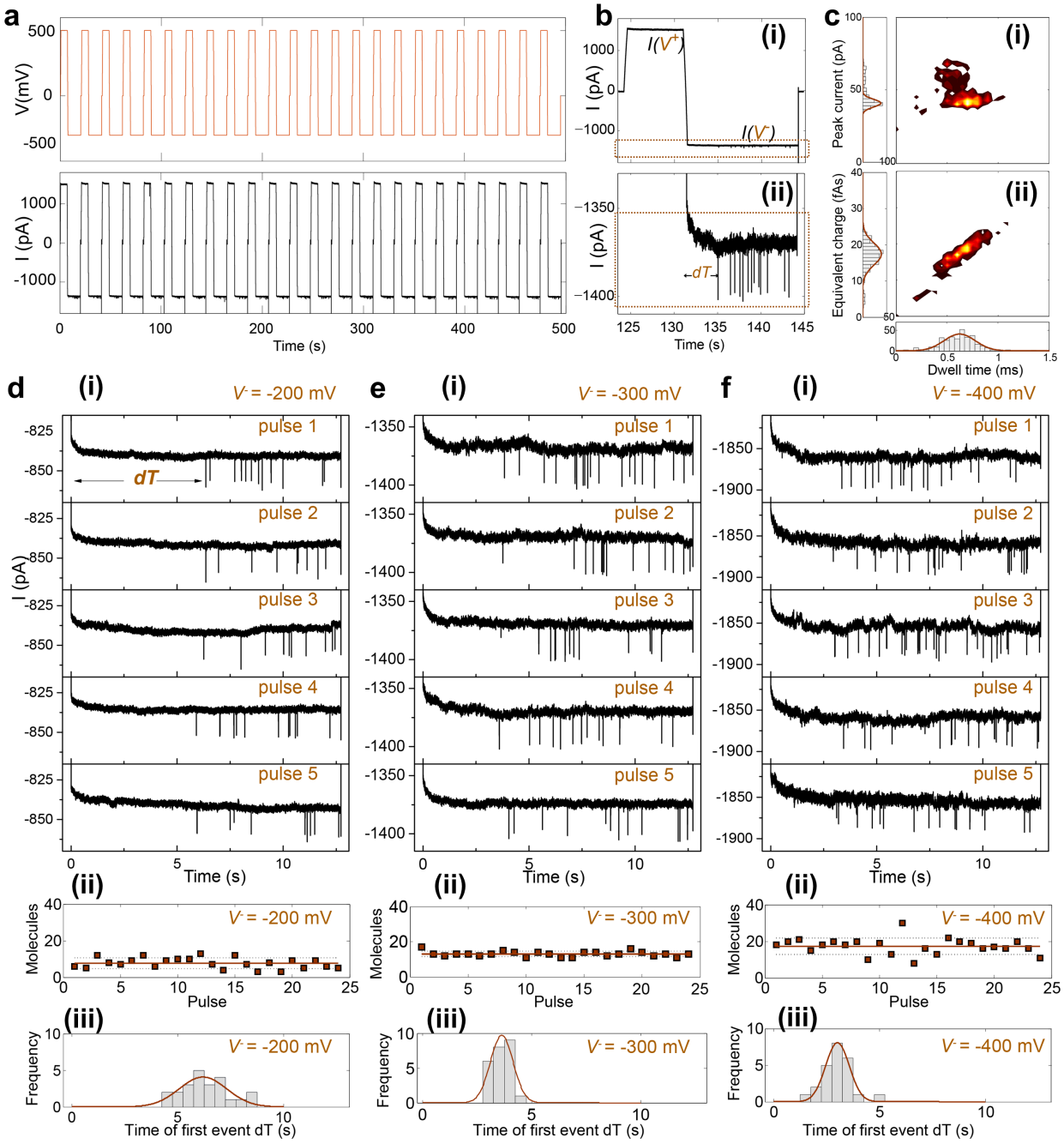

Figure 2 | Single molecule detection and delivery. **a,** *I-t* and *V-t* measurements of the first 500 s (24 delivery cycles) of 150 pM, 10 kbp DNA molecules, with V^+ =500 mV, V^- = -300 mV, t^+ = 6.4 s and t^- = 12.7 s. **b, (i)** A magnified view of a single cycle showing the *I-t* trace for V^+ and V^- pulses and **(ii)** and magnified view of the same current trace for V^- showing individual delivery events. **c, (i)** Event scatter plots of peak current (after baseline subtraction) versus dwell

time and (**ii**) equivalent charge vs dwell time for the 24 cycles show in **a**. At V = -300 mV the most probable pore dwell time is 0.6 ± 0.2 ms with a mean charge (integrated current area per translocation) of 18.0 ± 4.1 fAs, as calculated from the histogram fits. **d,e,f (i)** Representative *I-t* traces for delivery of 150 pM, 10 kbp DNA for V = -200 mV, V = -300 mV, V = -400 mV, respectively. For better visualization, the recordings were filtered digitally with a 1 KHz low-pass filter **(ii)** Data points showing the number of delivered DNA molecules per cycle. The orange solid line shows the average number of molecules delivered per cycle: 17.7±4.5 molecules at V = -400 mV, 13.1±3.3 molecules at V = -300 mV and 8.0 ± 3.0 molecules at V = -200 mV (mean value ± one standard deviation). **(iii)** Histogram showing the time distribution of the first event in a delivery cycle for the 24 delivery cycles. The first molecule is delivered faster at higher V

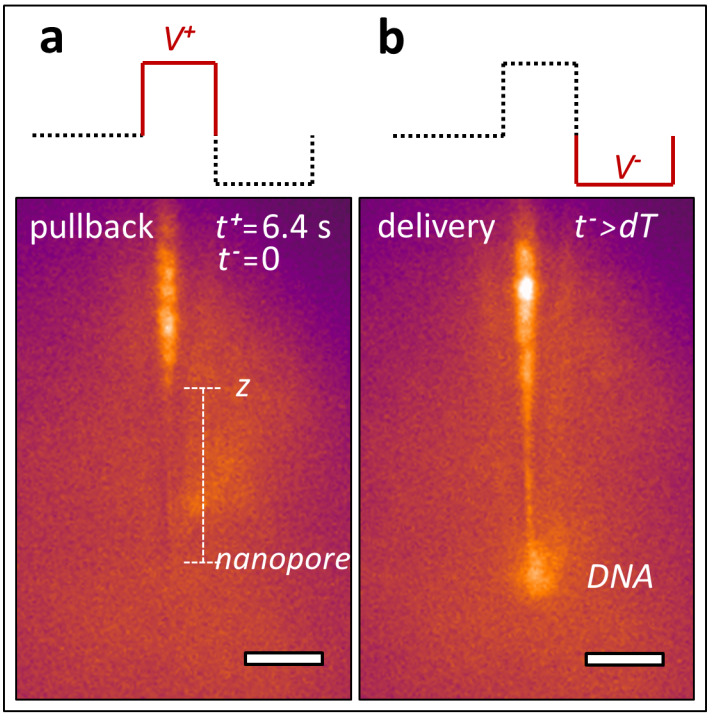

Figure 3 | Fluorescence imaging of DNA molecules at the nanopipette tip. a, Image of the tip at the end of a positive pulse (at t^{+}= 6.4 s) at $V = V^{+}$ = 500 mV, showing tip depletion of the DNA molecules to a position z from the tip of the nanopipette. In repeating pulse cycles the DNA molecules were pulled to the same position z (additional information is available in the Supporting Fig. 5 and Supporting Fig. 9) **b**, Image of the tip at $V = V^{-}$ = -300 mV at t^{-}= 5 s (t = 11.4 s), DNA is delivered through the nanopore at the tip of the nanopipette. The DNA sample was 1500 pM, 10 kbp, labeled with YOYO-1 fluorescent dye. All scale bars are 10 µm. A movie DNATrans.avi demonstrating the delivery process is shown in the supporting information.

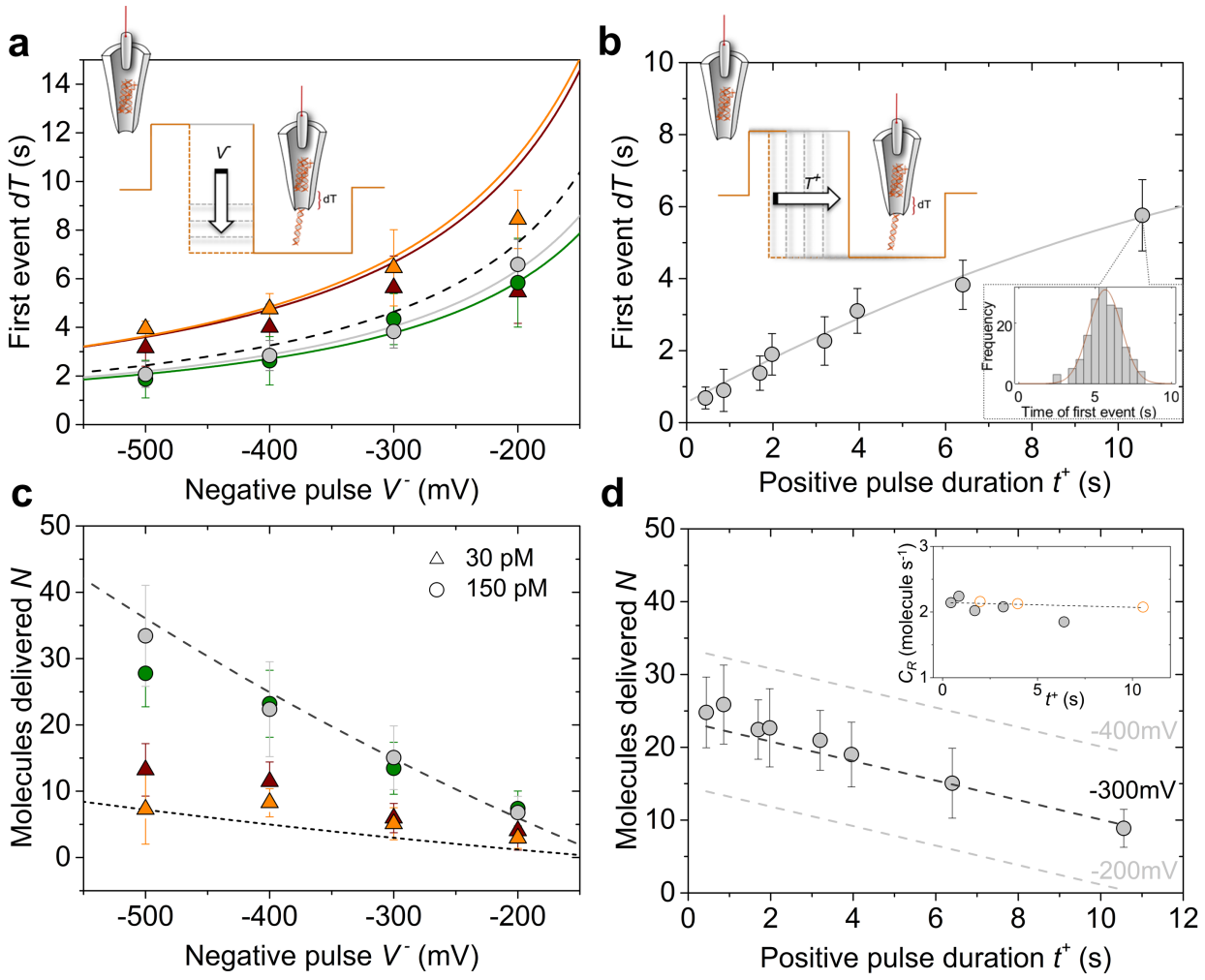

Figure 4 | Controllable delivery of DNA molecules. The time of the first event dT and the number of molecules delivered in a pulse is accurately controlled by varying the potentials V^+ and V^- and the positive pulse duration t^+. **a,** Experimentally measured times of the first event as a function of the applied potential V^- for 356 delivery pulses of 30 pM 10 kbp (orange triangles), 30 pM 5 kbp (red triangles), 150 pM 10 kbp (gray circles) and 150 pM 5 kbp DNA (green circles). The curves show theoretical values of dT from either time-dependent simulations (solid lines; color coded the same as the experimental data) and from eq (2) (dashed line). Both experiments and simulations have been carried out for positive pulses, V^+ = 500 mV and t^+ = 6.4 s. **b** Time of the first event as a function of t^+ for 150 pM 10 kbp DNA, with V^+ = 500 mV

and V^- = -300 mV. The solid line shows the predicted values of dT from time-dependent finite element simulations. The inset shows a histogram for the last data point (t^+ = 10.6 s) based on 168 consecutive measurements of dT. A total number of 5501 DNA molecules were delivered over 5700 s. **c,** Number of molecules, N, delivered in a negative pulse with a fixed duration (t^- = 12.7 s) for different negative pulse potentials V^- for of 30 pM 10 kbp (orange triangles), 30 pM 5 kbp (red triangles), 150 pM 10 kbp (gray circles) and 150 pM 5 kbp DNA (green circles), with predicted values of dT from eq (3), using eq (2) for dT, (dashed lines). **d,** Number of delivered molecules per pulse (t^- = 12.7 s) for different positive pulse durations t^+ (V^+ = 500 mV and V^- = -300 mV). (inset) DNA capture rate measurements for different positive pulse durations t^+ for t^- = 12.7 s (o) and t^- = 21.0 s (o). The dashed lines are theoretical values from eq (3) using eq (2) to calculate dT.

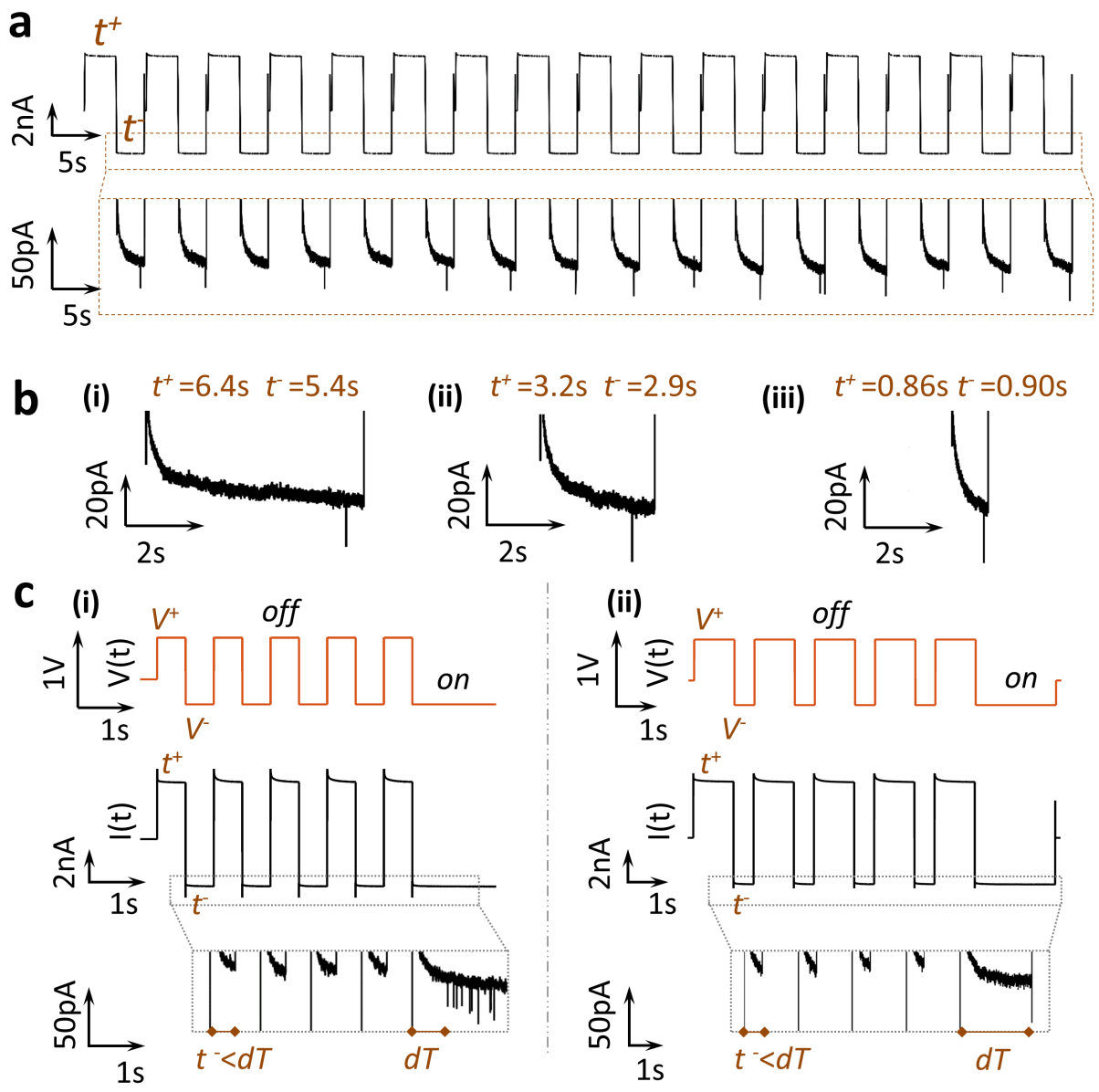

Figure 5 | Delivery of single DNA molecules. a, *I-t* trace showing 16 consecutive pulses (100 s in total) illustrating delivery of single DNA molecules (top panel) and a blow up of the events (lower panel) for 1500 pM 10 kbp DNA with V^+ = 500 mV, V^- = -300 mV, t^+ = 3.2 s and t^- = 2.9 s. **b,** Representative *I-t* pulses for different t^+ and t^- combinations, showing single molecule delivery in a pulse. Single molecules are delivered faster by using short t^+. **c,** Switching molecular delivery "on and off" on demand. Measured *V-t* and *I-t* pulses for 1500 pM, 10kbp

DNA with V^{+} = 500 mV and V^{-} = -300 mV. The bottom panel shows the blown up *I-t* trace. DNA molecules are pulsed back and forth in the nanopipette close to tip opening without being delivered when operated in the regime $t^{-} < dT$ (first four cycles). Molecular delivery is then achieved on-demand by switching to $t^{-} > dT$. **c$_{i}$** Multiple molecules are delivered on demand and **c$_{ii}$** single molecule delivered in a pulse.

References

1. Dekker, C. Solid-state nanopores. *Nature nanotechnology* 2007, 2, 209-215.
2. Venkatesan, B. M.; Bashir, R. Nanopore sensors for nucleic acid analysis. *Nature nanotechnology* 2011, 6, 615-624.
3. Miles, B. N.; Ivanov, A. P.; Wilson, K. A.; Dogan, F.; Japrung, D.; Edel, J. B. Single molecule sensing with solid-state nanopores: novel materials, methods, and applications. *Chemical Society reviews* 2013, 42, 15-28.
4. Wanunu, M.; Morrison, W.; Rabin, Y.; Grosberg, A. Y.; Meller, A. Electrostatic focusing of unlabelled DNA into nanoscale pores using a salt gradient. *Nature nanotechnology* 2010, 5, 160-165.
5. Ivanov, A. P.; Instuli, E.; McGilvery, C. M.; Baldwin, G.; McComb, D. W.; Albrecht, T.; Edel, J. B. DNA Tunneling Detector Embedded in a Nanopore. *Nano Letters* 2010, 11, 279-285.
6. Wei, R.; Gatterdam, V.; Wieneke, R.; Tampe, R.; Rant, U. Stochastic sensing of proteins with receptor-modified solid-state nanopores. *Nat Nanotechnol* 2012, 7, 257-63.
7. Storm, A. J.; Storm, C.; Chen, J. H.; Zandbergen, H.; Joanny, J. F.; Dekker, C. Fast DNA translocation through a solid-state nanopore. *Nano Letters* 2005, 5, 1193-1197.
8. Iqbal, S. M.; Akin, D.; Bashir, R. Solid-state nanopore channels with DNA selectivity. *Nat Nanotechnol* 2007, 2, 243-8.
9. Wanunu, M.; Bhattacharya, S.; Xie, Y.; Tor, Y.; Aksimentiev, A.; Drndic, M. Nanopore analysis of individual RNA/antibiotic complexes. *ACS Nano* 2011, 5, 9345-53.
10. Li, W.; Bell, N. A. W.; Hernandez-Ainsa, S.; Thacker, V. V.; Thackray, A. M.; Bujdoso, R.; Keyser, U. F. Single Protein Molecule Detection by Glass Nanopores. *Acs Nano* 2013, 7, 4129-4134.
11. Karhanek, M.; Kemp, J. T.; Pourmand, N.; Davis, R. W.; Webb, C. D. Single DNA Molecule Detection Using Nanopipettes and Nanoparticles. *Nano Letters* 2005, 5, 403-407.
12. Steinbock, L. J.; Otto, O.; Chimerel, C.; Gornall, J.; Keyser, U. F. Detecting DNA Folding with Nanocapillaries. *Nano Letters* 2010, 10, 2493-2497.
13. Li, W.; Bell, N. A. W.; Hernández-Ainsa, S.; Thacker, V. V.; Thackray, A. M.; Bujdoso, R.; Keyser, U. F. Single Protein Molecule Detection by Glass Nanopores. *ACS Nano* 2013, 7, 4129-4134.
14. Haywood, D. G.; Saha-Shah, A.; Baker, L. A.; Jacobson, S. C. Fundamental Studies of Nanofluidics: Nanopores, Nanochannels, and Nanopipets. *Anal Chem* 2014.
15. Novak, P.; Li, C.; Shevchuk, A. I.; Stepanyan, R.; Caldwell, M.; Hughes, S.; Smart, T. G.; Gorelik, J.; Ostanin, V. P.; Lab, M. J.; Moss, G. W. J.; Frolenkov, G. I.; Klenerman, D.; Korchev, Y. E. Nanoscale live-cell imaging using hopping probe ion conductance microscopy. *Nat Methods* 2009, 6, 279-281.
16. Actis, P.; Tokar, S.; Clausmeyer, J.; Babakinejad, B.; Mikhaleva, S.; Cornut, R.; Takahashi, Y.; Cordoba, A. L.; Novak, P.; Shevchuck, A. I.; Dougan, J. A.; Kazarian, S. G.; Gorelkin, P. V.; Erofeev, A. S.; Yaminsky, I. V.; Unwin, P. R.; Schuhmann, W.; Klenerman, D.; Rusakov, D. A.; Sviderskaya, E. V.; Korchev, Y. E. Electrochemical Nanoprobes for Single-Cell Analysis. *Acs Nano* 2014, 8, 875-884.
17. Knoblauch, M.; Hibberd, J. M.; Gray, J. C.; van Bel, A. J. E. A galinstan expansion femtosyringe for microinjection of eukaryotic organelles and prokaryotes. *Nat Biotechnol* 1999, 17, 906-909.

18. Bruckbauer, A.; James, P.; Zhou, D. J.; Yoon, J. W.; Excell, D.; Korchev, Y.; Jones, R.; Klenerman, D. Nanopipette delivery of individual molecules to cellular compartments for single-molecule fluorescence tracking. *Biophys J* 2007, 93, 3120-3131.
19. Singhal, R.; Orynbayeva, Z.; Sundaram, R. V. K.; Niu, J. J.; Bhattacharyya, S.; Vitol, E. A.; Schrlau, M. G.; Papazoglou, E. S.; Friedman, G.; Gogotsi, Y. Multifunctional carbon-nanotube cellular endoscopes. *Nature nanotechnology* 2011, 6, 57-64.
20. Adam Seger, R.; Actis, P.; Penfold, C.; Maalouf, M.; Vilozny, B.; Pourmand, N. Voltage controlled nano-injection system for single-cell surgery. *Nanoscale* 2012, 4, 5843-5846.
21. Babakinejad, B.; Jönsson, P.; López Córdoba, A.; Actis, P.; Novak, P.; Takahashi, Y.; Shevchuk, A.; Anand, U.; Anand, P.; Drews, A.; Ferrer-Montiel, A.; Klenerman, D.; Korchev, Y. E. Local Delivery of Molecules from a Nanopipette for Quantitative Receptor Mapping on Live Cells. *Analytical Chemistry* 2013, 85, 9333-9342.
22. Actis, P.; Maalouf, M. M.; Kim, H. J.; Lohith, A.; Vilozny, B.; Seger, R. A.; Pourmand, N. Compartmental genomics in living cells revealed by single-cell nanobiopsy. *ACS Nano* 2014, 8, 546-53.
23. Ying, L.; Bruckbauer, A.; Rothery, A. M.; Korchev, Y. E.; Klenerman, D. Programmable Delivery of DNA through a Nanopipet. *Analytical Chemistry* 2002, 74, 1380-1385.
24. Steinbock, L. J.; Lucas, A.; Otto, O.; Keyser, U. F. Voltage-driven transport of ions and DNA through nanocapillaries. *Electrophoresis* 2012, 33, 3480-3487.
25. Bell, N. A.; Thacker, V. V.; Hernandez-Ainsa, S.; Fuentes-Perez, M. E.; Moreno-Herrero, F.; Liedl, T.; Keyser, U. F. Multiplexed ionic current sensing with glass nanopores. *Lab on a chip* 2013, 13, 1859-62.
26. Gong, X.; Patil, A. V.; Ivanov, A. P.; Kong, Q.; Gibb, T.; Dogan, F.; deMello, A. J.; Edel, J. B. Label-free in-flow detection of single DNA molecules using glass nanopipettes. *Anal Chem* 2014, 86, 835-41.
27. Gibb, T. R.; Ivanov, A. P.; Edel, J. B.; Albrecht, T. Single Molecule Ionic Current Sensing in Segmented Flow Microfluidics. *Analytical Chemistry* 2014, 86, 1864-1871.
28. Wei, C.; Bard, A. J.; Feldberg, S. W. Current Rectification at Quartz Nanopipet Electrodes. *Analytical Chemistry* 1997, 69, 4627-4633.
29. Siwy, Z.; Fulinski, A. Fabrication of a synthetic nanopore ion pump. *Physical review letters* 2002, 89, 198103.
30. Lan, W.-J.; Holden, D. A.; White, H. S. Pressure-Dependent Ion Current Rectification in Conical-Shaped Glass Nanopores. *Journal of the American Chemical Society* 2011, 133, 13300-13303.
31. Sa, N.; Baker, L. A. Experiment and Simulation of Ion Transport through Nanopipettes of Well-Defined Conical Geometry. *J Electrochem Soc* 2013, 160, H376-H381.
32. Freedman, K. J.; Haq, S. R.; Fletcher, M. R.; Foley, J. P.; Jemth, P.; Edel, J. B.; Kim, M. J. Nonequilibrium Capture Rates Induce Protein Accumulation and Enhanced Adsorption to Solid-State Nanopores. *ACS Nano* 2014.
33. Smeets, R. M. M.; Keyser, U. F.; Krapf, D.; Wu, M.-Y.; Dekker, N. H.; Dekker, C. Salt Dependence of Ion Transport and DNA Translocation through Solid-State Nanopores. *Nano Letters* 2005, 6, 89-95.
34. Gershow, M.; Golovchenko, J. A. Recapturing and trapping single molecules with a solid-state nanopore. *Nature nanotechnology* 2007, 2, 775-779.

35. Plesa, C.; Cornelissen, L.; Tuijtel, M. W.; Dekker, C. Non-equilibrium folding of individual DNA molecules recaptured up to 1000 times in a solid state nanopore. *Nanotechnology* 2013, 24, 475101.
36. Kubeil, C.; Bund, A. The Role of Nanopore Geometry for the Rectification of Ionic Currents. *J Phys Chem C* 2011, 115, 7866-7873.
37. White, H. S.; Bund, A. Ion current rectification at nanopores in glass membranes. *Langmuir* 2008, 24, 2212-2218.
38. Ying, L.; White, S. S.; Bruckbauer, A.; Meadows, L.; Korchev, Y. E.; Klenerman, D. Frequency and voltage dependence of the dielectrophoretic trapping of short lengths of DNA and dCTP in a nanopipette. *Biophys J* 2004, 86, 1018-27.
39. Bruckbauer, A.; Zhou, D. J.; Ying, L. M.; Abell, C.; Klenerman, D. A simple voltage controlled enzymatic nanoreactor produced in the tip of a nanopipet. *Nano Letters* 2004, 4, 1859-1862.
40. Kirby, B. J.; Hasselbrink, E. F., Jr. Zeta potential of microfluidic substrates: 1. Theory, experimental techniques, and effects on separations. *Electrophoresis* 2004, 25, 187-202.
41. Chansin, G. A. T.; Mulero, R.; Hong, J.; Kim, M. J.; Demello, A. J.; Edel, J. B. Single-molecule Spectroscopy using nanoporous membranes. *Nano Letters* 2007, 7, 2901-2906.
42. Cecchini, M. P.; Wiener, A.; Turek, V. A.; Chon, H.; Lee, S.; Ivanov, A. P.; McComb, D. W.; Choo, J.; Albrecht, T.; Maier, S. A.; Edel, J. B. Rapid Ultrasensitive Single Particle Surface-Enhanced Raman Spectroscopy Using Metallic Nanopores. *Nano Letters* 2013, 13, 4602-4609.

Acknowledgements

J.B.E. has been funded in part by an ERC starting investigator grant and a BBSRC grant. PJ was supported by a grant from the Swedish Research Council (number: 623-2014-6387)

TOC Figure